

M. Riva, B. Esposito, D. Marocco, F. Belli, B. Syme  
and JET EFDA contributors

# The New Digital Electronics for the JET Neutron Profile Monitor: Performances and First Experimental Results

“This document is intended for publication in the open literature. It is made available on the understanding that it may not be further circulated and extracts or references may not be published prior to publication of the original when applicable, or without the consent of the Publications Officer, EFDA, Culham Science Centre, Abingdon, Oxon, OX14 3DB, UK.”

“Enquiries about Copyright and reproduction should be addressed to the Publications Officer, EFDA, Culham Science Centre, Abingdon, Oxon, OX14 3DB, UK.”

The contents of this preprint and all other JET EFDA Preprints and Conference Papers are available to view online free at [www.iop.org/Jet](http://www.iop.org/Jet). This site has full search facilities and e-mail alert options. The diagrams contained within the PDFs on this site are hyperlinked from the year 1996 onwards.

# The New Digital Electronics for the JET Neutron Profile Monitor: Performances and First Experimental Results

M. Riva<sup>1</sup>, B. Esposito<sup>1</sup>, D. Marocco<sup>1</sup>, F. Belli<sup>1</sup>, B. Syme<sup>2</sup>  
and JET EFDA contributors\*

*JET-EFDA, Culham Science Centre, OX14 3DB, Abingdon, UK*

<sup>1</sup>*Associazione Euratom-ENEA sulla Fusione, C.P. 65, Frascati I-00044, Roma (Italy)*

<sup>2</sup>*EURATOM-CCFE Fusion Association, Culham Science Centre, OX14 3DB, Abingdon, OXON, UK*

*\* See annex of F. Romanelli et al, "Overview of JET Results",  
(Proc. 22<sup>nd</sup> IAEA Fusion Energy Conference, Geneva, Switzerland (2008)).*

Preprint of Paper to be submitted for publication in Proceedings of the  
26th Symposium on Fusion Technology (SOFT), Porto, Portugal  
27th September 2010 - 1st October 2010



## **ABSTRACT.**

The 2D neutron emissivity profile is measured at JET by a set of NE213 liquid organic scintillators, located in two fan-shaped arrays of collimators with 10 horizontal and 9 vertical lines of sight. As the detectors are sensitive to neutron and gamma rays, pulse shape analysis is required for neutron/gamma discrimination. A digital architecture data-handling data acquisition and processing for the entire diagnostic has been developed by ENEA-Frascati and installed at JET during the 2009 campaign as a replacement of the existing analogue electronics. This paper describes the performances of the digital system and the first experimental results in the JET C27b campaign.

## **1. INTRODUCTION**

The JET Neutron Profile Monitor (NPM) [1,2], is designed for the measurement of the plasma neutron emissivity. It consists of two fan shaped arrays of collimators (10 horizontal + 9 vertical lines of sight (LOS)), where each LOS has a NE213 liquid scintillator for the detection of 2.5 MeV and 14MeV neutrons.

This paper describes the NPM digital acquisition/processing system that replaces the existing JET analogue electronics. The core of the new system is represented by the neutron/gamma (n/ $\gamma$ ) Digital Pulse shape discrimination (DPSD) acquisition boards providing the separation between the neutron and gamma events recorded by the scintillators.

The signals from the NPM NE213 scintillators are acquired by a set of five DPSD boards, each one with 4 acquisition channels (20 channels in total: 19+1 spare). Each channel has a 14 bit resolution with a 200MHz sampling rate. An interleaving technique is used, combining two channels @100MHz sampling rate. The overall noise, after a calibration procedure, is below -75 dB [3]. The main aims of the upgraded system are: production of n and  $\gamma$  count rates, production of n and  $\gamma$  pulse height spectra for each LOS on any preset time and energy window, high count rate operation (up to MHz range), raw data (i.e.: pulse signals) re-processing capability, real-time count rates for control and pile-up rejection & software correction.

The paper describes the main features of the system with particular focus on the real-time performance and presents preliminary results collected in plasma discharges during the C27b JET experimental campaign.

## **2. DPSD BOARD CHARACTERISTICS**

Figure 1 shows a picture of an acquisition board. It hosts four channels (controlled by two FPGAs), two Ethernet ports, two serial ports and various control signals.

Each DPSD acquisition board is fully configurable. Thanks to the Ethernet port and the embedded Linux operating system integrated in the FPGA, it is possible to set the parameters of the acquisition, to poll the state of the system as well as to start/stop the acquisitions. A server program running on the FPGA routes all requests to the appropriate hardware resources. A hardware version of the charge comparison method (see section 3.2) for the n/ $\gamma$  separation has been implemented in the

FPGA. The resulting real time  $n$  and  $\gamma$  output count rates are routed through the Ethernet port to a PC to be sent to the real time JET network using ATM (Asynchronous Transfer Mode) protocol. The main characteristics of the system are listed below.

### **2.1 EXTERNAL SAMPLING RATE MAIN CLOCK**

In order to avoid timing jitter between different boards it has been chosen to have a unique external, differential input clock source distributed to all boards. A separate clock generator and splitter has been developed and mounted at JET.

### **2.2 SERIAL PORT**

The CPU integrated in the FPGA has a serial port for system inspection and debugging, acting as a terminal for the CPU.

### **2.3 EXTERNAL JET CLOCK REFERENCE**

The system is normally synchronized with an internal 1 MHz clock to produce a precise time stamp for each acquired pulse. External clock synchronization with the JET reference clock is also possible.

### **2.4 RANDOM ACQUISITION MODE**

The acquisition is normally started on the pulse arrival (*internal trigger*). The option of triggering the acquisition using an *external trigger* is also available: this is useful for non-linearity checks on the ADCs.

### **2.5 DYNAMIC WINDOW DATA ACQUISITION**

The system adopts a Dynamic Window Data Acquisition (DWDA) technique [3], enabling the dynamic increase of the acquisition window size depending on the pulse duration and in presence of a new pulse at the end of the window. A comparison between the window length distributions obtained during  $\gamma$  calibration ( $^{22}\text{Na}$  source) and plasma discharges is shown in Fig.2. The effect of DWDA during the plasma discharge (when longer pulses due to neutrons and a non negligible fraction of pile-up events are present) is clearly seen. A fixed length acquisition option is also available.

### **2.6 BLOCK ACQUISITION**

A block acquisition feature (for acquisition of entire blocks of data regardless of the timing) is available. This is used for the calibration of the internal ADCs with sinusoidal signals.

## **3. BOARD PERFORMANCES**

The performances of the boards have been analyzed during the JET C27b campaign. Almost all plasma discharges for all 19 channels have been acquired locally on the four acquisition PCs. The signals from the photomultipliers are amplified ( $A=3$ ) in order to match the input range of the ADCs.

### **3.1 ACQUISITION**

The C27b campaign produced a total of  $\sim 0.5$  TBytes of data. For the central, higher pulse rate

channels (5 and 15), the average file size was  $\sim 200$  Mbytes/channel. This figure is well below the maximum foreseen value of 500 Mbytes/channel.

### **3.2 POST-PROCESSING**

The LabVIEW™ DPSD\_ENEA software [4,5] has been used to post-process the acquired data. The software evaluates separate n and  $\gamma$  pulse height spectra and count rates by applying the charge comparison method (i.e. by integrating each pulse in two different time intervals and evaluating their ratio). The pulse energy is evaluated by integration of the whole pulse. An example of n/ $\gamma$  separation is shown in Fig. 3.

### **3.3. REAL TIME**

The real time n/ $\gamma$  separation capabilities of the DPSD acquisition boards have been studied in laboratory using pulses from a programmable pulse generator (Fig.4).

The resulting distribution in the separation plot (Fig.5) has been arbitrarily divided in two populations to simulate n and  $\gamma$  events. The obtained real time and LabVIEW™ post-processing count rates for the two populations are shown in Fig. 6, indicating an agreement within 0.1% up to a total count rate of  $\sim 0.9$  MHz.

Another test has been made to evaluate the delay in the delivery of the real time packets from the FPGAs to the control PC. The packets are sent in small User Datagram Protocol (UDP) packets every ms. The UDP time for each packet is written in the packet by a hardware counter in the FPGA. The difference in arrival time between two consecutive packets ( $\Delta t = \text{UDP}(t=1) - \text{UDP}$ ) has been measured. The goal is to achieve  $\Delta t \leq 10\text{ms}$  for the whole set of 20 channels. The results, shown in Fig.7, are well within this limit. The maximum delay was found to be 5ms; the distribution of the time delays is centered on 1 ms for 99.99% of the events. Therefore, the real time count rates can be used for control purposes without any significant data loss.

As the PC Ethernet board is capable to handle 1 Gbit/s rate and each packet was about 30 bytes (in total 300 Kbytes/s) the actual bandwidth usage was about 2%.

## **4. C27B EXPERIMENTAL RESULTS**

A high neutron yield discharge (Pulse No: 79698, with  $I_p = 4.5\text{MA}$ ,  $B_t = 3.6\text{ T}$ ,  $P_{\text{NBI}} = 22.9\text{MW}$ ,  $P_{\text{ICRH}} = 2.6\text{MW}$ ,  $Y_n = \sim 1.5 \times 10^{16}$  n/s) has been selected to analyze the behaviour of the NPM new digital acquisition/processing system.

All LOS' have been energy calibrated using the built-in  $^{22}\text{Na}$   $\gamma$  source of each scintillator (the channels corresponding to the Compton edges of the two  $^{22}\text{Na}$  lines have been determined for all detectors). The n/ $\gamma$  separation plots (as in Fig.2) have been produced and count rates have been determined for the following proton energy ranges: 1.8–3.5MeV (to detect 2.5MeV neutrons (DD)), 3.5-10MeV (to detect neutrons due fast ion tails (FAST)), 10–16MeV (to detect 14MeV neutrons (DT)). Typical separation plots for the DD and DT energy windows (pulse height equivalent) are shown in Fig.8 (detector #4). The corresponding n and  $\gamma$  pulse height spectra are shown in Fig.9,

where the DD and DT edges are seen; also note that  $\gamma$  events are not present in the DT window.

Figure 10 shows the resulting count rates (20 ms integration time) for the DD windows from the horizontal camera (trace 3, LOS #1-10) compared with the total neutron rate from the fission chamber monitors and time traces of the ICRH and NBI power. In this discharge the pile-up correction factor has been measured to be at most  $\sim 10\%$  (no correction has been applied to the data shown in the figures).

The neutron radial profiles, respectively for the DD and DT energy windows, are shown in Fig.11 for several time slices (100 ms integration time). Note the different rise times of the DD and DT profiles (compare profiles at 49.5 and 50 s) due to the triton slowing down time. Fig.12 shows the comparison between the count rates in the DD, DT and FAST energy windows for detector #4: again, a delay in the raise of the FAST and DT signals can be observed.

## CONCLUSIONS AND FUTURE WORK

The JET Neutron Profile Monitor (NPM) has been upgraded with a digital data acquisition/processing system, which provides both real time and post-processed neutron and gamma count rates. Laboratory tests have proven that the real time n and  $\gamma$  count rates provided by the system are well within the JET time requirement (10 ms); moreover, they match the post-processed count rates within 0.1% up to 0.9 MHz (repetitive) pulse rate. The performances of the system have also been tested in deuterium plasma discharges during the JET C27b campaign. Total count rates up to  $\sim 2 \times 10^5$  counts/s have been sustained in the central vertical LOS. The boards perform correctly and provide n/ $\gamma$  separation, pulse height spectra and simultaneous 2.5MeV and 14MeV neutrons count rates. Preliminary radial neutron profiles have been also obtained. Future work includes an extensive data analysis of the data collected during the C27b campaign, the test of the real time system during plasma discharges and the implementation of a hard real time kernel in the FPGA.

## ACKNOWLEDGMENTS

This work was supported by EURATOM and carried out within the framework of the European Fusion Development Agreement. The views and opinions expressed herein do not necessarily reflect those of the European Commission.

## REFERENCES

- [1]. M. Adams et al., Nuclear Instruments and Methods in Physics Research **A329**, 277 (1993).
- [2]. O.N. Jarvis et al., Fusion Engineering and Design **34-35**, 59 (1997).
- [3]. M. Riva et al., Fusion Engineering and Design **82**, 1245 (2007).
- [4]. D. Marocco et al., PoS FNDA 2006 (028), <http://pos.sissa.it>, (2006)
- [5]. B. Esposito et al., Nuclear Instruments and Methods in Physics Research **A572**, 355 (2007).





Figure 1: Front panel of the DPSD acquisition board.

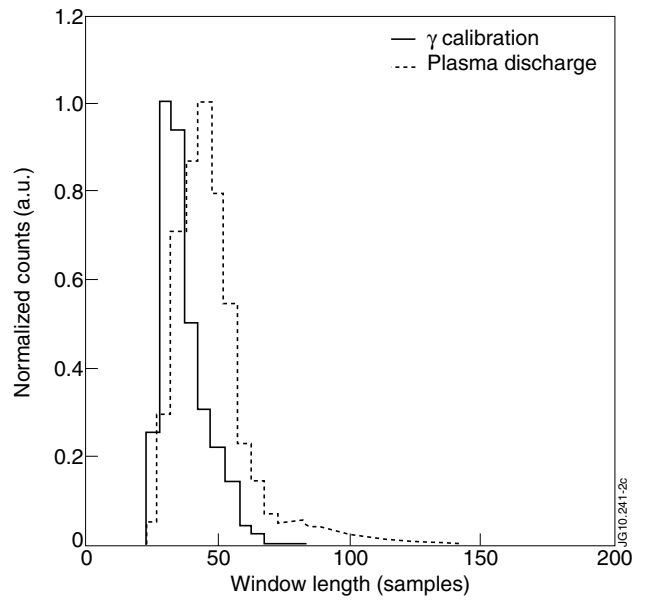


Figure 2: Typical data window length distributions (normalized to the peak value) for a  $\gamma$  calibration (solid) and for a plasma discharge (dashed).

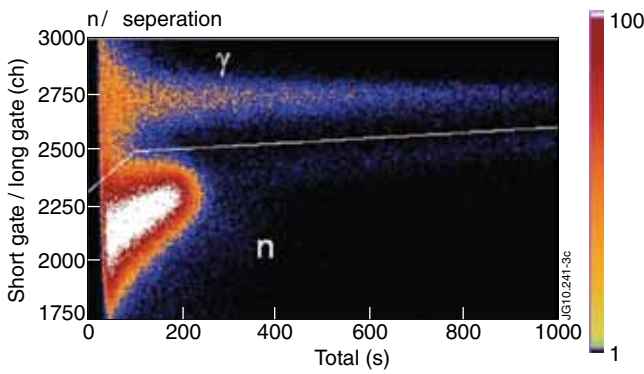


Figure 3: Typical  $n/\gamma$  separation plot for a JET plasma discharge. The white curve is the separation line; x-axis = pulse energy; y-axis = ratio of short to long time intervals.

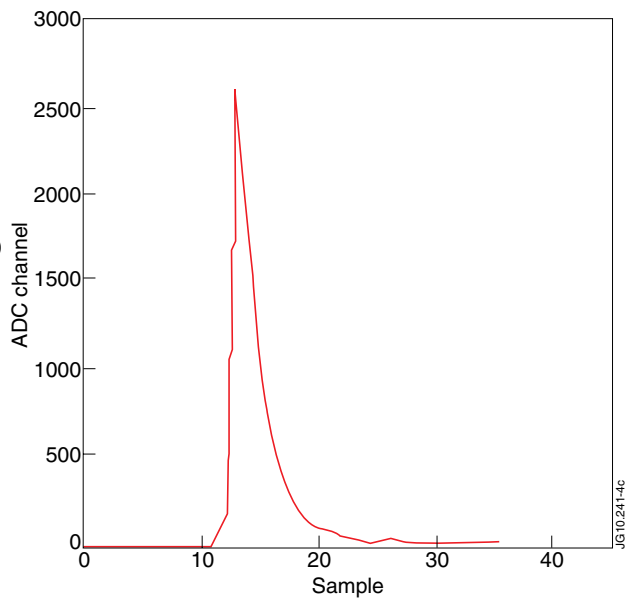


Figure 4: Typical pulse from the generator.

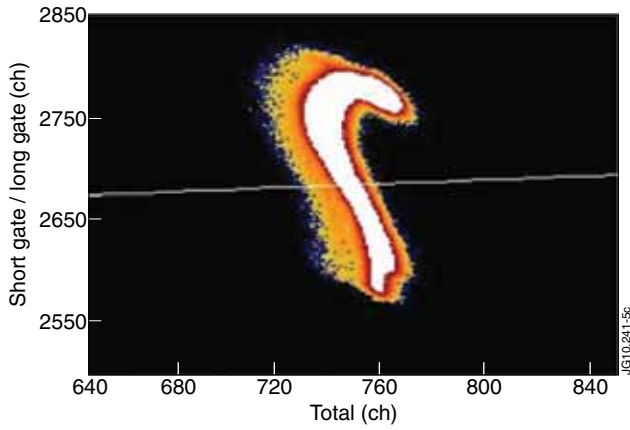


Figure 5: Separation plot of pulses from a programmable generator (x and y axes as in Fig.3).

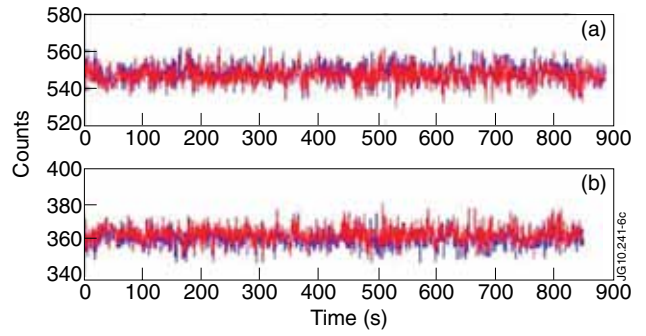


Figure 6: Comparison between count rates from real time (blue) and from LabView<sup>TM</sup> post-processing (red): a) upper population; b) lower population.

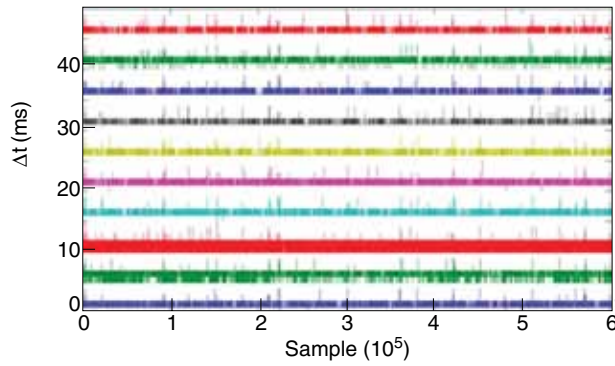


Figure 7: Difference between two consecutive arrival times of packets sent to the PC (for the 10 FPGA boards, shown with  $i*5ms$  ( $i=0,9$ ) offset on the y axis for clarity reasons). The acquisition lasts 600s. The maximum difference in time between packets is 5ms.

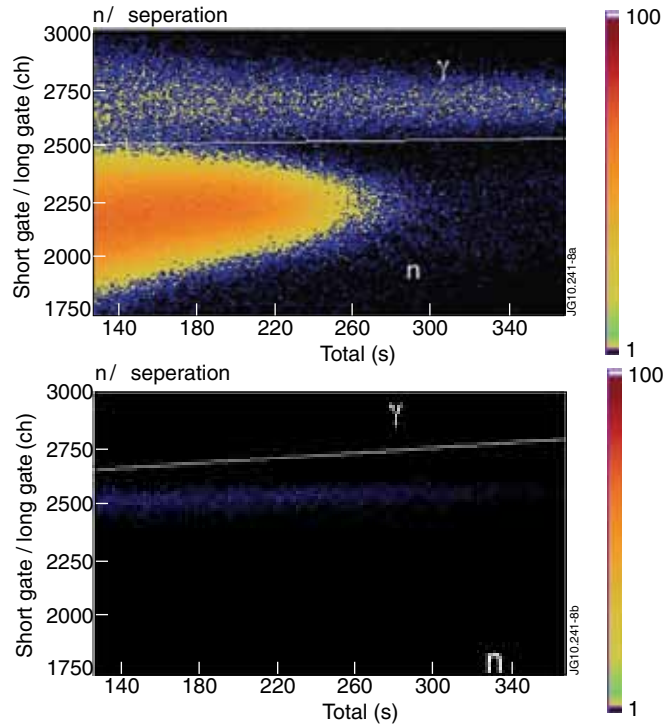


Figure 8:  $n/\gamma$  separation plots (DD (top) and DT (bottom) energy windows) for LOS #4 (Pulse No: 79698).

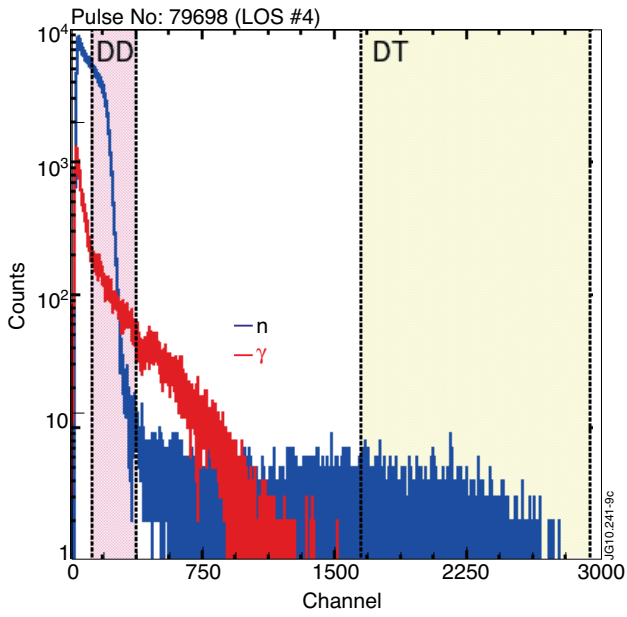


Figure 9:  $n$  and  $\gamma$  pulse height spectra for LOS #4 (Pulse No: 79698).

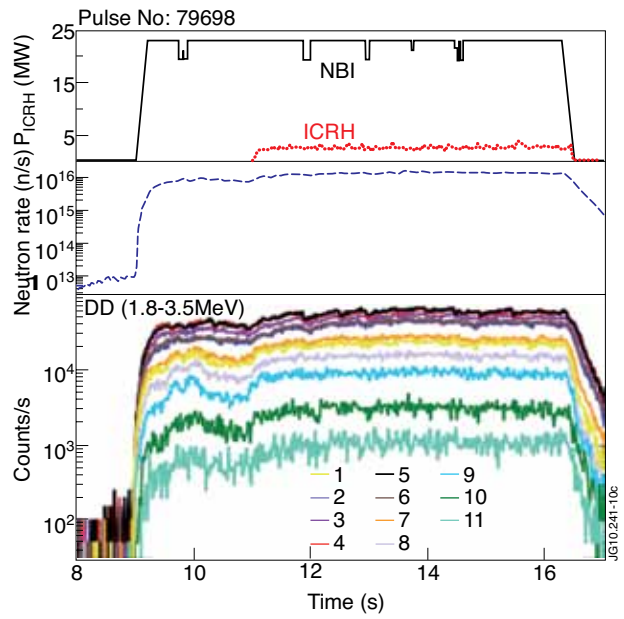


Figure 10: Time traces for Pulse No: 79698: a) ICRH and NBI power; b) total neutron rate; c) NPM horizontal LOS #1-10 (DD energy window).

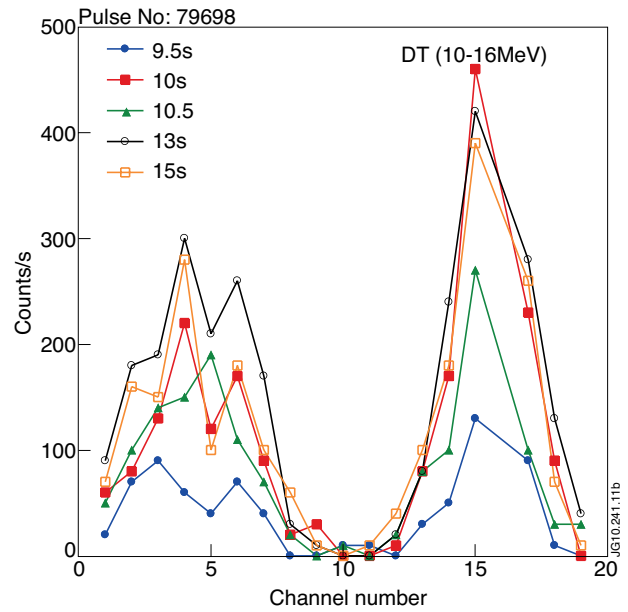
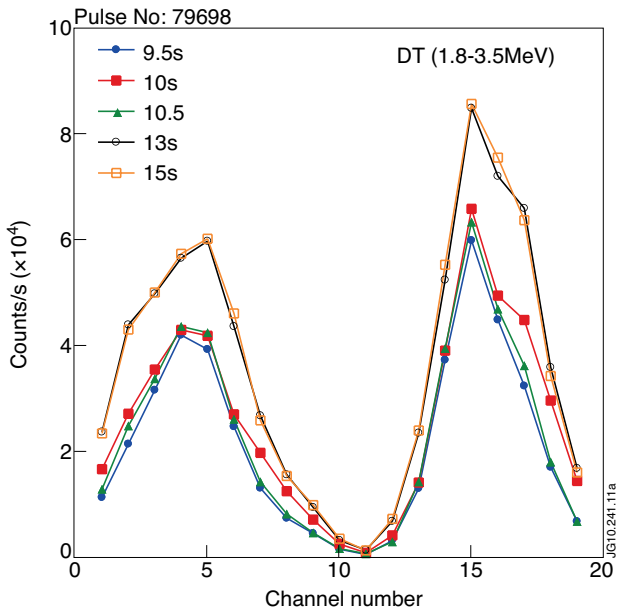


Figure 11: Neutron profiles for Pulse No: 79698: DD (top) and DT (bottom).

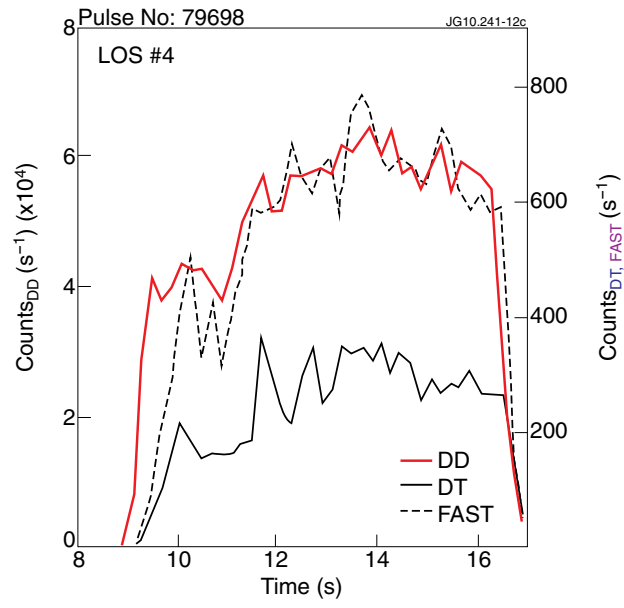


Figure 12: Neutron count rates (200ms integration time) for DD, DT and FAST energy windows (Pulse No: 79698).